

Spatial quantum error correction threshold

Ari Mizel *Laboratory for Physical Sciences, College Park, Maryland 20740, USA*

(Received 29 December 2022; accepted 10 January 2024; published 5 February 2024)

We consider a spatial analogue of the quantum error correction threshold. Given individual time-independent subsystems in which quantum information is coherent over sufficiently long lengths, we show how the information can be kept coherent for arbitrarily long lengths by forming time-independent composite systems. The subsystem coherence range exhibits threshold behavior. When it exceeds a range ξ_{th} , meaningful information can be extracted from the ground state of the composite system. Otherwise, the information is garbled. The threshold transition implies that the parent Hamiltonian of the ground state has gone from gapped to gapless. Ramifications of the construction for projected entangled pair states and for adiabatic quantum computation are considered.

DOI: [10.1103/PhysRevA.109.022406](https://doi.org/10.1103/PhysRevA.109.022406)

I. INTRODUCTION

The quantum error correction [1–4] threshold theorem [5–7] is a foundational element of the theory of quantum computation. Roughly, it shows that, provided a system has quantum gates with infidelity below a threshold value p_{th} , scalable computation is possible. The noise in the gates can be tamed using redundancy, by encoding physical qubits into logical qubits. Loosely speaking, if quantum information in individual subsystems remains coherent for sufficiently long times, it can be kept coherent for arbitrarily long times merely by forming composite systems.

In this paper, we consider the spatial analogue of this phenomenon. Given individual subsystems in which quantum information is coherent over sufficiently long lengths, can it be kept coherent for arbitrarily long lengths merely by forming composite systems? Is there spatial threshold behavior? In defining the question, it is important to emphasize that we are considering the properties of a *time-independent* quantum state. In the usual, temporal version of quantum error correction, it is often supposed that the qubits occupy different spatial locations. A set of time-dependent errors can therefore be visualized as occurring at a set of distinct positions, a perspective that is especially helpful in the context of topological codes [8]. However, this is only superficially similar to the question we are asking about time-independent spatial coherence.

To answer the question, we specify a quantum subsystem that serves as an elemental building block, analogous to a qubit in the usual quantum error correction context. Given any quantum circuit \mathbf{c} , it is possible to encode a fault-tolerant version of \mathbf{c} into the time-independent state $|\Psi(\theta)\rangle$ of an assembly of these subsystems. A parameter θ tunes the minimum coherence range $\xi(\theta)$ of the subsystems. We show that $\xi(\theta)$ exhibits spatial quantum error correction threshold behavior. When $\xi(\theta)$ is just over a threshold value ξ_{th} , the output of \mathbf{c} can be extracted from $|\Psi(\theta)\rangle$. Otherwise, the output of \mathbf{c} is generally too garbled to extract. Conveniently, $|\Psi(\theta)\rangle$ is

the ground state of a two-local [9] parent Hamiltonian $H(\theta)$. The construction leverages ground-state quantum computation [10–13] with important additional features from quantum error correction.

The paper is structured as follows. The bulk of the exposition spells out the construction of $|\Psi(\theta)\rangle$ and $H(\theta)$. We derive the threshold behavior as the coherence range $\xi(\theta)$ crosses just over ξ_{th} . Then, we show that there is a gapped to gapless transition in $H(\theta)$. Finally, we discuss implications of the construction for the theory of projected entangled pair states (PEPS) and for universal adiabatic quantum computation.

II. RESULTS

A. Building block

To describe the construction of $|\Psi(\theta)\rangle$, we assume that our starting quantum circuit \mathbf{c} is composed of only initializations and unitary gates. No midcircuit measurements occur, and we also exclude from the definition of \mathbf{c} final measurements to probe its output state; such final measurements are regarded as occurring immediately after \mathbf{c} has run to completion. We can encode physical qubits into logical qubits to form a fault-tolerant [5–7] quantum circuit \mathbf{C} . While measurements are often used within fault-tolerant circuits to extract entropy, this is inessential [5]; it will be convenient to assume that our circuit \mathbf{C} uses only initializations and one- and two-qubit unitary gates. The fault tolerance allows \mathbf{C} to produce the correct output of \mathbf{c} even in the presence of noise. In particular, we will use the fact that \mathbf{C} can produce the correct output of \mathbf{c} even if each of the gates of \mathbf{C} is followed with probability p by a depolarizing channel. It is only necessary that $p \leq p_{\text{th}} - \delta p$, where p_{th} is the quantum error correction threshold and δp is fixed and positive.

The map from \mathbf{C} to $|\Psi(\theta)\rangle$ is most easily described using explicit circuit examples as shown in Fig. 1. For each example, we will also specify a two-local parent Hamiltonian $H(\theta)$ as a sum of initialization terms H_{init} , one-qubit gate terms $H_{\text{one}}^U(\theta)$, and two-qubit gate terms $H_{\text{two}}^W(\theta)$ in one-to-one correspondence with the initializations, one-qubit gates, and two-qubit gates of \mathbf{C} . The Hamiltonian is represented symbolically in Fig. 2.

*ari@arimizel.com

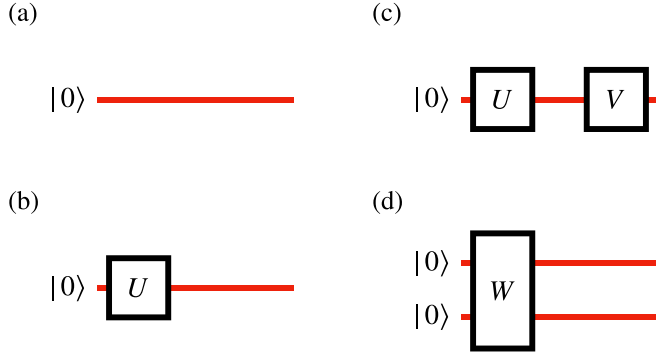


FIG. 1. Example circuits, with time flowing to the right. (a) Trivial circuit composed solely of initialization without any gates. (b) Initialization of a qubit, followed by a one-qubit gate U . (c) Circuit (b) followed by a second one-qubit gate, V . (d) Initialization of two qubits followed by a two-qubit gate.

Start with the trivial circuit in Fig. 1(a) that simply initializes a qubit. Define a two-dimensional Hilbert space with basis $\{|0_0\rangle, |1_0\rangle\}$ where the ket $|b_s\rangle$ has “bit” value b and computational “stage” value s . For the trivial circuit of Fig. 1(a), there is only stage $s = 0$, and the desired time-independent state is $|0_0\rangle$. It is the zero-energy ground state of the positive semidefinite parent Hamiltonian $H_{\text{init}} = \epsilon|1_0\rangle\langle 1_0|$ with ϵ a fixed energy scale. Figure 2(a) depicts H_{init} symbolically.

To apply a one-qubit gate U to the qubit after initialization, as in Fig. 1(b), extend its two-dimensional Hilbert space so that it has dimension $2 \otimes 3 \otimes (1 \oplus 2 \oplus 2)$. We will explain this extension in two steps. Consider first extending from a two-dimensional space to a $2 \oplus 2$ -dimensional space, replacing the original basis $\{|0_0\rangle, |1_0\rangle\}$ with an extended basis $\{|0_1\rangle, |1_1\rangle\} \cup \{|0_0\rangle, |1_0\rangle\}$. The time-independent state of the qubit in this extended space is assigned the form $\frac{1}{\sqrt{2}}(|0_1\rangle\langle 0|U|0\rangle + |1_1\rangle\langle 1|U|0\rangle + |0_0\rangle)$, where $\langle 0|U|0\rangle$ and $\langle 1|U|0\rangle$ are matrix elements of the one-qubit gate U . This state of the qubit is a superposition of computational stage $s = 0$ after initialization and stage $s = 1$ after U is applied. In this way, we use superposition to replicate time evolution within a time-independent state. If we define the operator $\mathcal{U} = \sum_{b,\beta,s=0,1} |b_s\rangle\langle b|U|\beta\rangle\langle\beta_s|$ that applies U while keeping the stage fixed, then our state can be written in the compact form

$$\frac{1}{\sqrt{2}}(\mathcal{U}|0_1\rangle + |0_0\rangle). \quad (1)$$

This state captures the action of U , but it has the unacceptable property that the postgate output $U|0\rangle$ is present with an amplitude of just $\frac{1}{\sqrt{2}}$. This is reminiscent of qubit leakage in standard time-dependent quantum computation, in which an external disturbance ejects a qubit from its two-dimensional Hilbert space. However, here we have the peculiar feature that the qubit is sometimes at the wrong instant of “time,” occupying the state $|0_0\rangle$ associated with stage $s = 0$ of the computation rather than the desired state $\mathcal{U}|0_1\rangle$ associated with stage $s = 1$ of the computation. At first, this kind of “leakage in time” seems like an inevitable consequence of the fact that we are using superposition to replicate time evolution within a time-independent state. However, it turns out that we

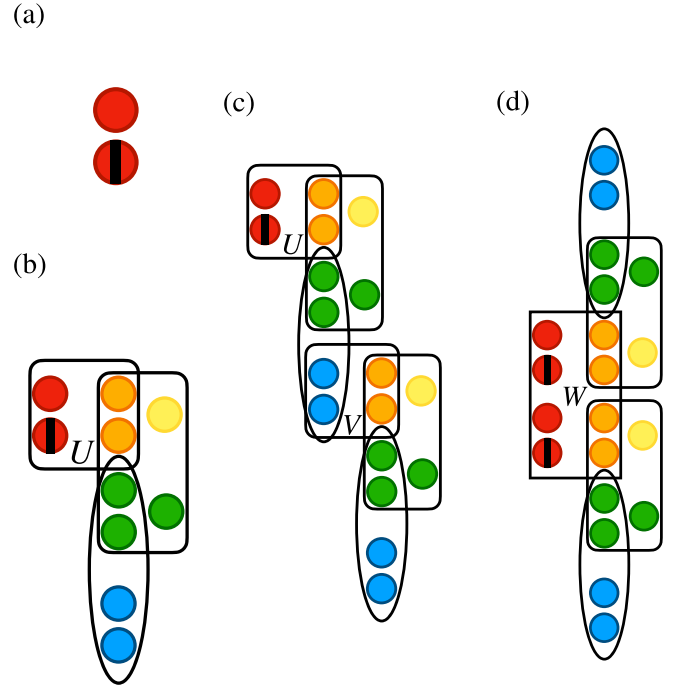


FIG. 2. Graphical depiction of Hamiltonians corresponding to circuits in Fig. 1, with space flowing to the right rather than time. (a) A pair of circles represents the two states $\{|0_0\rangle, |1_0\rangle\}$. Concretely, one can think of an electron shared between quantum dots or a Cooper pair shared between superconducting islands. The vertical black line represents the energy penalty H_{init} . (b) To apply a gate U , the two-dimensional Hilbert space is extended to $2 \otimes 3 \otimes (1 \oplus 2 \oplus 2)$ dimensions. Colored circles represent the associated basis states according to the correspondence blue \otimes green \otimes (yellow \oplus orange \oplus red). The terms of $H_{\text{one}}^U(\theta)$ are depicted using a square outline to represent Eq. (9), a rectangle for (11), and an oval for (10). (c) To apply a second gate V , the leftmost part of the $2 \otimes 3 \otimes (1 \oplus 2 \oplus 2)$ -dimensional space is extended, yielding a $2 \otimes 3 \otimes (1 \oplus 2 \oplus 2) \otimes 3 \otimes (1 \oplus 2 \oplus 2)$ -dimensional space. (d) Analogue of (b) for a two-qubit gate W .

can eliminate this leakage-in-time error, trading it for depolarization error that can be subdued using standard quantum error correction.

To make this trade, we extend the space of the qubit from $2 \oplus 2$ dimensional to $2 \otimes 3 \otimes (1 \oplus 2 \oplus 2)$ dimensional. This allows us to incorporate a teleportationlike step [14] acting after U . Figure 2(b) is color coded in consonance with the teleportation circuit in Fig. 3 to clarify the role of each part of the $2 \otimes 3 \otimes (1 \oplus 2 \oplus 2)$ -dimensional Hilbert space. A convenient basis for the Hilbert space is $\{|0_0\rangle, |1_0\rangle\} \otimes \{\text{IDLE}, |0_0\rangle, |1_0\rangle\} \otimes (\{\text{IDLE}\} \cup \{|0_1\rangle, |1_1\rangle\} \cup \{|0_0\rangle, |1_0\rangle\})$. Our state is assigned the form $|\psi^U(0)\rangle$ where

$$\begin{aligned} |\psi^U(b)\rangle = & \sqrt{\frac{2}{8 \cos^2 \theta + \sin^2 \theta}} \\ & \times [\cos \theta (|0_0\rangle \otimes |0_0\rangle + |1_0\rangle \otimes |1_0\rangle) \otimes (\mathcal{U}|b_1\rangle \\ & + |b_0\rangle) + \sin \theta \mathcal{U}|b_0\rangle \otimes \text{IDLE} \otimes \text{IDLE}] / \sqrt{2} \end{aligned} \quad (2)$$

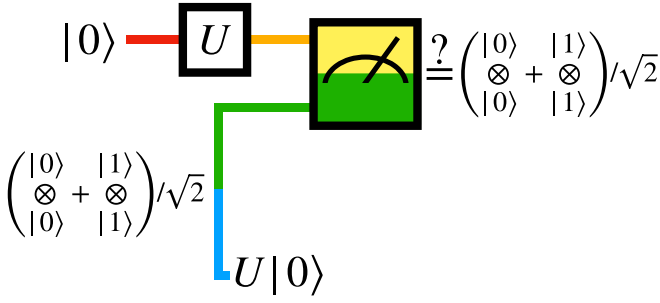


FIG. 3. Teleportation circuit. A postselection step checks that the measured state is $(|0\rangle \otimes |0\rangle + |1\rangle \otimes |1\rangle)/\sqrt{2}$; when this is true, the outgoing state on the bottom is $U|0\rangle$. The color coding shows the correspondence between the parts of the circuit and the parts of Fig. 2(b).

for $b = 0, 1$. In the first term of $|\psi^U(b)\rangle$, we prepend, alongside a state $(\mathcal{U}|b_1\rangle + |b_0\rangle)/\sqrt{2}$ like (1), a Bell pair $(|0_0\rangle \otimes |0_0\rangle + |1_0\rangle \otimes |1_0\rangle)$ needed for teleportation. The second term $\mathcal{U}|b_0\rangle \otimes |\text{IDLE}\rangle \otimes |\text{IDLE}\rangle$ completes teleportation, consuming the original qubit state and half of the Bell pair, so that the quantum information teleports to the other half of the Bell pair. (The label “IDLE” was chosen to suggest that the $3 \otimes (1 \oplus 2 \oplus 2)$ -dimensional part of the Hilbert space is in a neutral postmeasurement status, no longer carrying a qubit value $|0\rangle$ or $|1\rangle$.) State (2) completely resolves the leakage-in-time error suffered by state (1). In both terms of (2), the leftmost part of the $2 \otimes 3 \otimes (1 \oplus 2 \oplus 2)$ occupies a strictly two-dimensional Hilbert space spanned by the basis $\{|0_0\rangle, |1_0\rangle\}$. Granted, it is not always in the desired state $\mathcal{U}|b_0\rangle$; this is the cost of resolving the leakage-in-time error. Fortunately, when the parameter θ is close to $\pi/2$, the postgate output $U|b\rangle$ is available with an amplitude approaching 1 and the fidelity of the teleportation is high.

To formalize this in a useful way, we compute the density matrix of the system and trace out the $3 \otimes (1 \oplus 2 \oplus 2)$ -dimensional part. First, we define the one-qubit “gate operator”

$$\hat{g}_{\text{one}}^U = |\psi^U(0)\rangle\langle 0_0| + |\psi^U(1)\rangle\langle 1_0| \quad (3)$$

in terms of (2). This operator is a mapping from a two-dimensional space to a $2 \otimes 3 \otimes (1 \oplus 2 \oplus 2)$ -dimensional space. Our qubit state is simply $|\psi^U(0)\rangle = \hat{g}_{\text{one}}^U|0_0\rangle$ given in (2). Next, we define the superoperator

$$g_{\text{one}}^U(\rho) = \text{Tr}_{3 \otimes (1 \oplus 2 \oplus 2)} \hat{g}_{\text{one}}^U \rho \hat{g}_{\text{one}}^{U\dagger}. \quad (4)$$

One calculates that

$$g_{\text{one}}^U(\rho) = (1 - p_{\text{one}}) \mathcal{U} \rho \mathcal{U}^\dagger + p_{\text{one}} \text{Tr} \rho \frac{I^{(2)}}{2} \quad (5)$$

where

$$p_{\text{one}}(\theta) = \frac{8 \cos^2 \theta}{8 \cos^2 \theta + \sin^2 \theta} \quad (6)$$

and $I^{(k)}$ denotes the identity operator on a k -dimensional Hilbert space. Thus, $g_{\text{one}}^U(\rho)$ applies U followed by a depolarizing channel with probability p_{one} . The reduced density matrix of the leftmost two-dimensional part of the $2 \otimes 3 \otimes (1 \oplus 2 \oplus 2)$ -dimensional space of the qubit is $g_{\text{one}}^U(|0_0\rangle\langle 0_0|)$.

This yields the desired output $U|0\rangle$ of Fig. 1(b) with high probability as θ approaches $\pi/2$.

The $2 \otimes 3 \otimes (1 \oplus 2 \oplus 2)$ -dimensional subsystem is the elemental building block of our construction. The two states (2) are structured so that, in some sense, a 2×2 input density matrix ρ ends up becoming $g_{\text{one}}^U(\rho)$ as one moves spatially from one part of the subsystem to the other.

B. Coherence range

If we assume that the quantum state is distributed spatially like the dots laid out in Fig. 2(b), it is natural to define a coherence range describing the decay of quantum coherence from the rightmost two-dimensional part of the $2 \otimes 3 \otimes (1 \oplus 2 \oplus 2)$ -dimensional Hilbert space to the leftmost two-dimensional part. In the case of a one-qubit gate like we have been considering, we denote the coherence range $\xi_{\text{one}}(\theta)$. Since qubits are equivalent to spin-1/2 degrees of freedom, we define $\xi_{\text{one}}(\theta)$ using a kind of spin-spin correlation function. Denote the Pauli matrices by σ^i for $i = 1, 2, 3$. Let $\tau^i = \sum_{b,b'} |\psi^U(b)\rangle \sigma_{b,b'}^i \langle \psi^U(b')|$ express the Pauli matrix σ^i in the space $\{|\psi^U(b)\rangle | b \in 0, 1\}$ indexed by the pregate input b . Let $\zeta^i = (\sum_{b,b'} \mathcal{U}|b_0\rangle \sigma_{b,b'}^i \langle b_0| \mathcal{U}^\dagger) \otimes I^{(3)} \otimes (I^{(1)} \oplus I^{(2)} \oplus I^{(2)})$ express the Pauli matrix σ^i in the postgate output basis $\{\mathcal{U}|0_0\rangle, \mathcal{U}|1_0\rangle\}$. Define the spin-spin correlation function between input and output:

$$e^{-\frac{1}{\xi_{\text{one}}(\theta)}} = \frac{\text{Tr} \rho (\zeta^1 \tau^1 + \zeta^2 \tau^2 + \zeta^3 \tau^3)}{3} = 1 - p_{\text{one}}(\theta) \quad (7)$$

where $\rho = \sum_{b,b'} |\psi^U(b)\rangle \rho_{b,b'} \langle \psi^U(b')|$ denotes any density matrix with $\text{Tr} \rho = 1$. Note that the result is independent of U and ρ . As the depolarizing channel probability $p_{\text{one}}(\theta)$ grows, the coherence range $\xi_{\text{one}}(\theta)$ shrinks.

C. Parent Hamiltonian

We can find a positive semidefinite parent Hamiltonian

$$H_{\text{one}}^U(\theta) + I^{(2)} \otimes I^{(3)} \otimes H_{\text{init}}$$

that has $g_{\text{one}}^U|0_0\rangle$ as a nondegenerate zero-energy ground state. Earlier, we defined $H_{\text{init}} = \epsilon|1_0\rangle\langle 1_0|$. In a slight abuse of notation, we retain the same notation even though the operator above was defined on a two-dimensional Hilbert space with basis $\{|0_0\rangle, |1_0\rangle\}$, whereas now $H_{\text{init}} = \epsilon|1_0\rangle\langle 1_0|$ is defined on a $1 \oplus 2 \oplus 2$ -dimensional Hilbert space with basis $\{|\text{IDLE}\rangle \cup \{|0_1\rangle, |1_1\rangle\} \cup \{|0_0\rangle, |1_0\rangle\}$. We set

$$H_{\text{one}}^U(\theta) = I^{(2)} \otimes I^{(3)} \otimes H^U + H_B \otimes (I^{(1)} \oplus I^{(2)} \oplus I^{(2)}) + I^{(2)} \otimes H_P(\theta). \quad (8)$$

Figure 2(b) sketches the Hamiltonian, emphasizing the domain of each of these terms. The three operators H^U , H_B , and $H_P(\theta)$ take the following forms. First,

$$H^U = \epsilon \sum_b (\mathcal{U}|b_1\rangle - |b_0\rangle)(\langle b_1| \mathcal{U}^\dagger - \langle b_0|) / 2 \quad (9)$$

enforces the action of the specific unitary U . It is defined on a $1 \oplus 2 \oplus 2$ -dimensional Hilbert space. The Bell-pair term

$$H_B = \frac{\epsilon}{2} [(|1_0\rangle|0_0\rangle - |0_0\rangle|1_0\rangle)(\langle 1_0|\langle 0_0| - \langle 0_0|\langle 1_0|) \\ + (|1_0\rangle|0_0\rangle + |0_0\rangle|1_0\rangle)(\langle 1_0|\langle 0_0| + \langle 0_0|\langle 1_0|) \\ + (|0_0\rangle|0_0\rangle - |1_0\rangle|1_0\rangle)(\langle 0_0|\langle 0_0| - \langle 1_0|\langle 1_0|)] \quad (10)$$

imposes an energy penalty if the Bell pair in the first term of (2) is not of the desired form $(|0_0\rangle \otimes |0_0\rangle + |1_0\rangle \otimes |1_0\rangle)/\sqrt{2}$. It is defined on a $2 \otimes 3$ -dimensional Hilbert space. Finally, the projection term

$$H_P(\theta) = \epsilon \\ \times \left[\left(\sin \theta \frac{|0_0\rangle|0_1\rangle + |1_0\rangle|1_1\rangle}{\sqrt{2}} - \cos \theta |\text{IDLE}\rangle|\text{IDLE}\rangle \right) \right. \\ \times \left(\sin \theta \frac{\langle 0_0|\langle 0_1| + \langle 1_0|\langle 1_1|}{\sqrt{2}} - \cos \theta \langle \text{IDLE}|\langle \text{IDLE}| \right) \\ + |\text{IDLE}\rangle\langle \text{IDLE}| \otimes \sum_{b,s=0,1} |b_s\rangle\langle b_s| \\ \left. + \sum_{b=0,1} |b_0\rangle\langle b_0| \otimes |\text{IDLE}\rangle\langle \text{IDLE}| \right] \quad (11)$$

is designed to replace the Bell-basis measurement step of teleportation. In place of the Bell-basis measurement step of teleportation, it enforces a time-independent form of postselection on the states (2). The parameter θ is introduced to govern the relative contributions of the premeasurement and postmeasurement stages of the computation [i.e., the two terms in Eq. (2)]. The final lines of (11) impose an energy penalty unless both targets of the measurement undergo the step in tandem. The operator H_P is defined on a $3 \otimes (1 \oplus 2 \oplus 2)$ -dimensional Hilbert space.

D. Composing building blocks

We have discussed the state and parent Hamiltonian associated with a single one-qubit gate. To handle more complicated circuits, the construction of Fig. 2(b) can be iterated. For instance, if a second unitary gate V is applied to our qubit, as in Fig. 1(c), the ground state is assigned the form

$$[\hat{g}_{\text{one}}^V \otimes I^{(3)} \otimes (I^{(1)} \oplus I^{(2)} \oplus I^{(2)})] |\psi^U(0)\rangle \\ = [\hat{g}_{\text{one}}^V \otimes I^{(3)} \otimes (I^{(1)} \oplus I^{(2)} \oplus I^{(2)})] \hat{g}_{\text{one}}^U |0_0\rangle. \quad (12)$$

The action of \hat{g}_{one}^V iteratively expands the leftmost two-dimensional part of the Hilbert space, so that, instead of a $2 \otimes 3 \otimes (1 \oplus 2 \oplus 2)$ -dimensional space, the qubit now inhabits a $2 \otimes 3 \otimes (1 \oplus 2 \oplus 2) \otimes 3 \otimes (1 \oplus 2 \oplus 2)$ -dimensional space. The reduced density matrix of the leftmost two-dimensional Hilbert space is $g_{\text{one}}^V(g_{\text{one}}^U(|0_0\rangle\langle 0_0|))$. This equals the output produced by a noisy quantum circuit that starts with $|0\rangle$, applies U followed by a depolarizing channel with probability $p_{\text{one}}(\theta)$, then applies V followed by a depolarizing channel with probability $p_{\text{one}}(\theta)$. The Hamiltonian, depicted symbolically

in Fig. 2(c), is

$$H_{\text{one}}^V(\theta) \otimes I^{(3)} \otimes (I^{(1)} \oplus I^{(2)} \oplus I^{(2)}) + I^{(2)} \otimes I^{(3)} \otimes \\ \times [H_{\text{one}}^U(\theta) + (I^{(1)} \oplus I^{(2)} \oplus I^{(2)}) \otimes I^{(3)} \otimes H_{\text{init}}]. \quad (13)$$

It is worth reflecting on the essential role that teleportation plays in the construction presented in this paper. In the absence of teleportation, it is still possible to generalize (1) to include another gate. The natural generalization would take the form $\frac{1}{\sqrt{3}}(\mathcal{V}U|0_2\rangle + U|0_1\rangle + |0_0\rangle)$. The problem is that the postgate result $\mathcal{V}U|0_2\rangle$ appears with an amplitude of just $1/\sqrt{3}$ in this state. Effectively, leakage in time of quantum information, discussed above after Eq. (1), gets worse and worse with the addition of every gate. In contrast, when we include teleportation, the leakage-in-time problem goes away entirely, albeit with the cost that every gate is followed by a depolarization channel.

To incorporate the effect of a two-qubit gate W in \mathbf{C} , as in Fig. 1(d), \hat{g}_{one}^U is replaced with an operator \hat{g}_{two}^W . This is specified in detail in Appendix A. Its associated superoperator g_{two}^W applies W followed by a depolarizing channel on one or both qubits with probability

$$p_{\text{two}}(\theta) = \frac{32 \cos^4 \theta + 8 \cos^2 \theta \sin^2 \theta}{32 \cos^4 \theta + 8 \cos^2 \theta \sin^2 \theta + \sin^4 \theta}. \quad (14)$$

The Hamiltonian $H_{\text{two}}^W(\theta)$ is represented in Fig. 2(d). The coherence range $\xi_{\text{two}}(\theta)$ associated with the two-qubit gate is defined in analogy to (7), as described in Appendix B.

By iterating the constructions above, employing $2 \otimes 3 \otimes (1 \oplus 2 \oplus 2)$ -dimensional subsystems for each of the gates in \mathbf{C} , one obtains a $|\Psi(\theta)\rangle$ that contains the output of \mathbf{C} , and one also obtains the parent Hamiltonian $H(\theta)$ of $|\Psi(\theta)\rangle$. The state has the form $|\Psi(\theta)\rangle = \dots \hat{g}_{\text{two}}^W \dots \hat{g}_{\text{one}}^U \dots |0_0\rangle^{\otimes Q}$ where there is an operator of the form \hat{g}_{two}^W for each two-qubit gate in \mathbf{C} , there is an operator of the form \hat{g}_{one}^U for each one-qubit gate in \mathbf{C} , and Q is the number of qubits in \mathbf{C} . We have omitted tensor products with identity operators, abbreviating, for example, $[\hat{g}_{\text{one}}^V \otimes I^{(3)} \otimes (I^{(1)} \oplus I^{(2)} \oplus I^{(2)})]$ in (12) as \hat{g}_{one}^V . The final reduced density matrix of dimension $2^{\otimes Q}$, obtained by tracing out all but the final two-dimensional Hilbert space of each qubit, takes the abbreviated form $\dots (g_{\text{two}}^W \{ \dots g_{\text{one}}^U [\dots (|0_0\rangle\langle 0_0|^{\otimes Q}) \dots] \dots)$, where again we have omitted tensor products with identity operators. This equals the density matrix that would be produced by executing the quantum circuit \mathbf{C} with each perfect one-qubit unitary followed by depolarization with probability $p_{\text{one}}(\theta)$ and each perfect two-qubit unitary followed by depolarization with probability $p_{\text{two}}(\theta)$. Because $p_{\text{one}}(\theta) \leq p_{\text{two}}(\theta)$, we set the gate error probability p to $p_{\text{two}}(\theta)$. Then, \mathbf{C} 's fault tolerance implies the output of \mathbf{c} can be extracted, by decoding the final density matrix of dimension $2^{\otimes Q}$ of $|\Psi(\theta)\rangle$, provided $p_{\text{two}}(\theta) \leq p_{\text{th}} - \delta p$.

E. Threshold

This gives rise to our spatial quantum error correction threshold. We set the minimum coherence range $\xi(\theta)$ to $\xi_{\text{two}}(\theta)$ because $\xi_{\text{two}}(\theta) \leq \xi_{\text{one}}(\theta)$. When

$$\xi_{\text{two}}(\theta) \geq \xi_{\text{th}} + \delta \xi, \quad (15)$$

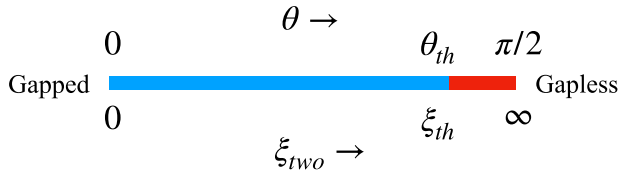


FIG. 4. Phase diagram of $H(\theta)$. Values of θ appear above the line with the corresponding value of ξ_{two} below. As ξ_{two} increases from zero to ∞ , it crosses the threshold value ξ_{th} , and the ground state develops long-range entanglement. This implies the Hamiltonian has become gapless.

the output of \mathbf{c} can be extracted. Here, ξ_{th} is defined as $\xi_{th} = \xi_{two}(\theta_{th})$ where $p_{two}(\theta_{th}) = p_{th}$, and $\delta\xi = \xi_{two}[p_{two}^{-1}(p_{th} + \delta p)] - \xi_{th}$.

When $\xi(\theta)$ crosses the threshold, there are ramifications for the properties of $H(\theta)$. A key property of interest is the energy gap, which is computed by taking the limit of large system size. Since the form of $H(\theta)$ is determined by a fault-tolerant circuit \mathbf{C} , this thermodynamic limit should be taken by specifying a family of larger and larger fault-tolerant circuits. One natural family is composed of circuits associated with a given quantum algorithm of growing problem size. However, it is simpler to consider [15] a circuit \mathbf{c} that starts with two qubits initialized to $|0\rangle \otimes |0\rangle$, applies a Hadamard gate to the second qubit to produce $|0\rangle \otimes (|0\rangle + |1\rangle)/\sqrt{2}$, and then applies a controlled-NOT (CNOT) gate targeting the first qubit in order to produce the Bell pair $(|0\rangle \otimes |0\rangle + |1\rangle \otimes |1\rangle)/\sqrt{2}$. Finally, a string of G identity gates is applied to each qubit of the pair. To take the limit of large system size, let G grow, with the fault-tolerant circuit \mathbf{C} requiring ever bulkier logical qubits.

At the point $\theta = 0$, where $\xi(\theta) = 0$, the energy eigenvalues of $H(\theta)$ are easily obtained by inspecting the forms of $H_{one}^U(\theta)$ and $H_{two}^W(\theta)$. We find a gap for all G . Now, $H(\theta)$ is going to remain gapped for small values of θ , but, by the time $\xi(\theta)$ crosses $\xi_{th} + \delta\xi$, the system must have undergone a transition to a gapless phase (see Fig. 4). This must happen because \mathbf{C} successfully outputs an intact logical Bell pair for all values of G . Thus, the ground state $|\Psi(\theta)\rangle$ contains long-range entanglement between the members of this Bell pair, which can only happen if $H(\theta)$ is gapless [16,17]. The argument is suitably generalized to other circuits \mathbf{C} in Appendix C.

III. DISCUSSION

We have demonstrated a spatial quantum error correction threshold. It is realized in the time-independent ground state $|\Psi(\theta)\rangle$ of a parent Hamiltonian $H(\theta)$. The threshold behavior is associated with a gapped to gapless transition in $H(\theta)$.

The results have interesting implications for the study of spatial correlations in quantum states, especially ground states, a topic that has been under active investigation in recent years [16–20]. Our construction demonstrates an unexpected

way in which quantum error correction, a tool that is proving to be remarkably versatile [21–25], can impact the analysis of such correlations. In particular, the gapped to gapless transition that we have exhibited is of significance in the context of PEPS [26–29] since $|\Psi(\theta)\rangle$ can be written as a projected entangled pair state (see Appendix D). While one-dimensional PEPS, referred to as matrix product states, generally have gapped parent Hamiltonians [30], understanding when higher-dimensional PEPS parent Hamiltonians are gapped and when they are gapless is a subtle problem under active consideration [31]. Our $|\Psi(\theta)\rangle$ and $H(\theta)$ provide a useful example to inform this investigation.

Moreover, the construction presented in this paper could be considered for use in universal adiabatic quantum computing [32]. Adiabatic quantum computing entails a system controlled by a parameter-dependent Hamiltonian $H(\theta)$. The Hamiltonian is designed so that $H(\theta_i)$ has a simple ground state while $H(\theta_f)$ has a useful ground state that can be measured to obtain the results of some computation. The ground state of $H(\theta_i)$ is the initial state of the computation. By slowly tuning θ from θ_i to θ_f , one adiabatically carries the initial state to the useful ground state of $H(\theta_f)$. In the construction detailed in this paper, by adiabatically carrying the parent Hamiltonian $H(\theta)$ from $\theta_i = 0$ to a θ_f close to $\pi/2$, one brings its ground state $|\Psi(\theta)\rangle$ from a simple initial form to one containing the output of \mathbf{c} .

There are a number of sources of error that can disrupt an adiabatic quantum computation.

(i) One source of error stems from the inevitable differences between the desired form of $H(\theta)$ and the form of $H(\theta)$ that ends up getting realized in an actual physical system.

(ii) Another source of error arises from thermal excitations of $H(\theta)$ out of its ground state as a result of the fact that the environment does not have zero temperature in the real world.

(iii) Related to this, we have a source of error that stems from leakage of the qubits of the physical system out of their Hilbert space as a result of environmental disturbances. It is noteworthy that the parent Hamiltonian $H(\theta)$ we have specified allows universal adiabatic quantum computation that is fault tolerant against sources of error (i) and (iii) as a result of the fault tolerance of the circuit \mathbf{c} . However, the gapless property of $H(\theta)$ indicates that, in thermal equilibrium, the system is not fault tolerant against thermal error (ii).

ACKNOWLEDGMENTS

The author gratefully acknowledges helpful discussions with M. B. Hastings, M. Kruger, D. A. Lidar, K. Miller, V. Molino, K. D. Osborn, V. N. Smelyanskiy, and M. M. Wilde.

APPENDIX A: TWO-QUBIT GATES

This section completes the discussion of Fig. 2(d), detailing the case of a two-qubit gate W . The two participating qubits inhabit a $[2 \otimes 3 \otimes (1 \oplus 2 \oplus 2)] \otimes [2 \otimes 3 \otimes (1 \oplus 2 \oplus 2)]$ -dimensional Hilbert space. We define four states of the

system by

$$\begin{aligned}
|\psi_0^W(b, B)\rangle &= \frac{1}{\sqrt{32 \cos^4 \theta + 8 \cos^2 \theta \sin^2 \theta + \sin^4 \theta}} \\
&\times \left[4 \cos^2 \theta \frac{1}{\sqrt{2}} (|0_0\rangle|0_0\rangle + |1_0\rangle|1_0\rangle) |b_0\rangle \frac{1}{\sqrt{2}} (|0_0\rangle|0_0\rangle + |1_0\rangle|1_0\rangle) |B_0\rangle \right. \\
&+ \sum_{b', B'} \langle b' | \langle B' | W | b \rangle | B \rangle \left(4 \cos^2 \theta \frac{1}{\sqrt{2}} (|0_0\rangle|0_0\rangle + |1_0\rangle|1_0\rangle) |b'_1\rangle \frac{1}{\sqrt{2}} (|0_0\rangle|0_0\rangle + |1_0\rangle|1_0\rangle) |B'_1\rangle \right. \\
&+ 2 \cos \theta \sin \theta |b'_0\rangle |IDLE\rangle |IDLE\rangle \frac{1}{\sqrt{2}} (|0_0\rangle|0_0\rangle + |1_0\rangle|1_0\rangle) |B'_1\rangle \\
&+ 2 \cos \theta \sin \theta \frac{1}{\sqrt{2}} (|0_0\rangle|0_0\rangle + |1_0\rangle|1_0\rangle) |b'_1\rangle |B'_0\rangle |IDLE\rangle |IDLE\rangle \\
&\left. \left. + \sin^2 \theta |b'_0\rangle |IDLE\rangle |IDLE\rangle |B'_0\rangle |IDLE\rangle |IDLE\rangle \right) \right]. \tag{A1}
\end{aligned}$$

In this equation, line 1 contains the normalization constant. Line 2 corresponds to the stage of the computation before W is applied. The input qubit states $|b\rangle$ and $|B\rangle$ are each accompanied by a Bell pair $(|0_0\rangle|0_0\rangle + |1_0\rangle|1_0\rangle)/\sqrt{2}$ that will be needed for teleportation. At line 3, W has been applied, but teleportation has not yet occurred, so the Bell pairs are still present. At lines 4 and 5, teleportation has occurred for one of the two qubits but not the other. At line 6, teleportation has occurred for both qubits, completing the gate.

The gate operator is defined by $\hat{g}_{\text{two}}^W = \sum_{b, B} |\psi_0^W(b, B)\rangle \langle b_0 | \langle B_0 |$. The corresponding superoperator is

$$\begin{aligned}
\hat{g}_{\text{two}}^W(\rho) &= \text{Tr}_{3 \otimes (1 \oplus 2 \oplus 2)} \text{Tr}_{3 \otimes (1 \oplus 2 \oplus 2)} \hat{g}_{\text{two}}^W \rho \hat{g}_{\text{two}}^{W\dagger} = [1 - p_{\text{two}}(\theta)] \mathcal{W} \rho \mathcal{W}^\dagger \\
&+ \frac{4 \cos^2 \theta \sin^2 \theta}{32 \cos^4 \theta + 8 \cos^2 \theta \sin^2 \theta + \sin^4 \theta} \sum_{b, B, B'} \langle b | \langle B | \rho | b' \rangle | B \rangle \mathcal{W} \left(|b_0\rangle \langle b'_0| \otimes \frac{|0_0\rangle \langle 0_0| + |1_0\rangle \langle 1_0|}{2} \right) \mathcal{W}^\dagger \\
&+ \frac{4 \cos^2 \theta \sin^2 \theta}{32 \cos^4 \theta + 8 \cos^2 \theta \sin^2 \theta + \sin^4 \theta} \sum_{b, B, B'} \langle b | \langle B | \rho | b \rangle | B' \rangle \mathcal{W} \left(\frac{|0_0\rangle \langle 0_0| + |1_0\rangle \langle 1_0|}{2} \otimes |B_0\rangle \langle B'_0| \right) \mathcal{W}^\dagger \\
&+ \frac{32 \cos^4 \theta}{32 \cos^4 \theta + 8 \cos^2 \theta \sin^2 \theta + \sin^4 \theta} \text{Tr} \rho \frac{|0_0\rangle \langle 0_0| + |1_0\rangle \langle 1_0|}{2} \otimes \frac{|0_0\rangle \langle 0_0| + |1_0\rangle \langle 1_0|}{2} \tag{A2}
\end{aligned}$$

with

$$p_{\text{two}}(\theta) = \frac{32 \cos^4 \theta + 8 \cos^2 \theta \sin^2 \theta}{32 \cos^4 \theta + 8 \cos^2 \theta \sin^2 \theta + \sin^4 \theta}.$$

Here, $\mathcal{W} = \sum_{s, b, B, b', B'} |b_s\rangle |B_s\rangle \langle b | \langle B | W | b' \rangle | B' \rangle \langle b'_s | \langle B'_s |$ applies W while keeping the stage variable fixed. The second line of Eq. (A2) corresponds to the successful application of the gate W . In the third and fourth lines, a depolarization channel has been applied to just one of the two qubits. In the final line, depolarization channels have been applied to both qubits. In Fig. 2(d), the reduced density matrix of the two qubits, after tracing out the $3 \otimes (1 \oplus 2 \oplus 2)$ -dimensional part of the Hilbert space of each, is $g_{\text{two}}^W(|0_0\rangle|0_0\rangle \langle 0_0| \langle 0_0|)$. This yields the desired output $W|0\rangle|0\rangle$ of Fig. 1(d) as θ approaches $\pi/2$.

The parent Hamiltonian of the ground states (A1) has the form

$$\begin{aligned}
H_{\text{two}}^W(\theta) &= \frac{\epsilon}{2} \sum_{b, B} I^{(2)} \otimes I^{(3)} \otimes |b_0\rangle \langle b_0| \otimes [I^{(2)} \otimes I^{(3)} \otimes |B_0\rangle \langle B_0|] \\
&+ \frac{\epsilon}{2} \sum_{b, B} [I^{(2)} \otimes I^{(3)} \otimes |b_1\rangle \langle b_1|] \otimes [I^{(2)} \otimes I^{(3)} \otimes |B_1\rangle \langle B_1|] \\
&- \frac{\epsilon}{2} \sum_{b, B, b', B'} \langle b' | \langle B' | W | b \rangle | B \rangle [I^{(2)} \otimes I^{(3)} \otimes |b'_1\rangle \langle b_0|] \otimes [I^{(2)} \otimes I^{(3)} \otimes |B'_1\rangle \langle B_0|] \\
&- \frac{\epsilon}{2} \sum_{b, B, b', B'} \langle b | \langle B | W^\dagger | b' \rangle | B' \rangle [I^{(2)} \otimes I^{(3)} \otimes |b_0\rangle \langle b'_1|] \otimes [I^{(2)} \otimes I^{(3)} \otimes |B_0\rangle \langle B'_1|] \\
&+ \frac{\epsilon}{2} [I^{(2)} \otimes I^{(3)} \otimes \sum_b |b_0\rangle \langle b_0|] \otimes [I^{(2)} \otimes I^{(3)} \otimes (|IDLE\rangle \langle IDLE| + \sum_B |B_1\rangle \langle B_1|)]
\end{aligned}$$

$$\begin{aligned}
 & + \frac{\epsilon}{2} [I^{(2)} \otimes I^{(3)} \otimes (|\text{IDLE}\rangle\langle\text{IDLE}| + \sum_b |b_1\rangle\langle b_1|)] \otimes [I^{(2)} \otimes I^{(3)} \otimes \sum_B |B_0\rangle\langle B_0|] \\
 & + [H_B \otimes (I^{(1)} \oplus I^{(2)} \oplus I^{(2)}) + I^{(2)} \otimes H_P] \otimes [I^{(2)} \otimes I^{(3)} \otimes (I^{(1)} \oplus I^{(2)} \oplus I^{(2)})] \\
 & + [I^{(2)} \otimes I^{(3)} \otimes (I^{(1)} \oplus I^{(2)} \oplus I^{(2)})] \otimes [H_B \otimes (I^{(1)} \oplus I^{(2)} \oplus I^{(2)}) + I^{(2)} \otimes H_P]. \tag{A3}
 \end{aligned}$$

The first four lines are analogous to the single-qubit gate case (9), despite superficial complexity resulting from the tensor product notation. Both qubits move together from stage 0 to stage 1, undergoing the gate W . The next two lines impose an energy penalty if either qubit attempts to traverse the gate alone. The seventh line is concerned with the teleportation of one qubit, and the final line is concerned with the teleportation of the other qubit. These last two lines employ the Hamiltonians (10) and (11).

The circuit in Fig. 1(d) includes initializations. Thus, the total Hamiltonian for Fig. 2(d) is

$$\begin{aligned}
 H(\theta) = & H_{\text{two}}^W(\theta) + [I^{(2)} \otimes I^{(3)} \otimes (I^{(1)} \oplus I^{(2)} \oplus I^{(2)})] \otimes [I^{(2)} \\
 & \otimes I^{(3)} \otimes H_{\text{init}}] + [I^{(2)} \otimes I^{(3)} \otimes H_{\text{init}}] \\
 & \otimes [I^{(2)} \otimes I^{(3)} \otimes (I^{(1)} \oplus I^{(2)} \oplus I^{(2)})]. \tag{A4}
 \end{aligned}$$

APPENDIX B: COHERENCE RANGES $\xi_{\text{one}}(\theta)$ AND $\xi_{\text{two}}(\theta)$

In this section, we first compute the coherence range $\xi_{\text{one}}(\theta)$ relation given in (7). It is convenient to define

$$\tilde{\sigma}^i = \sum_{b,b'} |b_0\rangle \sigma_{b,b'}^i \langle b'_0|, \tag{B1}$$

an operator corresponding to the Pauli matrix σ^i in the $|b_0\rangle$ basis. This definition implies that $\zeta^i = \mathcal{U} \tilde{\sigma}^i \mathcal{U}^\dagger$ and that $\tau^i = \hat{g}_{\text{one}}^U \tilde{\sigma} \hat{g}_{\text{one}}^{U\dagger}$. We also define

$$\tilde{\rho} = \sum_{b,b'} |b_0\rangle \rho_{b,b'} \langle b'_0|, \tag{B2}$$

an operator corresponding to the density matrix ρ in the $|b_0\rangle$ basis, so that $\rho = \hat{g}_{\text{one}}^U \tilde{\rho} \hat{g}_{\text{one}}^{U\dagger}$. We define $\xi_{\text{one}}(\theta)$ in terms of a kind of spin-spin correlation function:

$$\begin{aligned}
 e^{-1/\xi_{\text{one}}(\theta)} & = \frac{\text{Tr} \rho \left[\sum_{i=1}^3 \zeta^i \tau^i \right]}{3} \\
 & = \frac{\text{Tr} \left[\sum_{i=1}^3 \mathcal{U} \tilde{\sigma}^i \mathcal{U}^\dagger \hat{g}_{\text{one}}^U (\tilde{\sigma}^i \tilde{\rho}) \right]}{3} \\
 & = \frac{\text{Tr} \left[\sum_{i=1}^3 \tilde{\sigma}^i (1 - p_{\text{one}}(\theta)) \tilde{\sigma}^i \tilde{\rho} \right]}{3} \\
 & = 1 - p_{\text{one}}(\theta). \tag{B3}
 \end{aligned}$$

In the second equality, we have taken the trace over the $3 \otimes (1 \oplus 2 \oplus 2)$ parts of the $2 \otimes 3 \otimes (1 \oplus 2 \oplus 2)$ Hilbert space. In the third equality, we have used the formula $\hat{g}_{\text{one}}^U (\tilde{\sigma}^i \tilde{\rho}) = (1 - p_{\text{one}}) \mathcal{U} \tilde{\sigma}^i \tilde{\rho} \mathcal{U}^\dagger + p_{\text{one}} \text{Tr}(\tilde{\sigma}^i \tilde{\rho}) I/2$ that appears in the main text.

The definition of $\xi_{\text{one}}(\theta)$ can be extended to the case of a two-qubit gate W . The Hilbert space has dimension $2 \otimes 3 \otimes$

$(1 \oplus 2 \oplus 2) \otimes 2 \otimes 3 \otimes (1 \oplus 2 \oplus 2)$. Define $\zeta^{ij} = \mathcal{W}[\tilde{\sigma}^i \otimes I \otimes I \otimes \tilde{\sigma}^j \otimes I \otimes I] \mathcal{W}^\dagger$ where the two-qubit operator \mathcal{W} acts on the first and fourth parts of the Hilbert space:

$$\begin{aligned}
 \mathcal{W} & = \sum_{b,B,b',B'} \langle b| \langle B| \mathcal{W} |b'\rangle |B'\rangle \\
 & \times |b_0\rangle \langle b'_0| \otimes I \otimes I \otimes |B_0\rangle \langle B'_0| \otimes I \otimes I. \tag{B4}
 \end{aligned}$$

The subsystem spin operator is

$$\begin{aligned}
 \tau^{ij} & = \sum_{b,B,b',B'} |\psi_0^W(b,B)\rangle \sigma_{b,b'}^i \sigma_{B,B'}^j \langle \psi_0^W(b',B')| \\
 & = \hat{g}_{\text{two}}^W \tilde{\sigma}^i \otimes \tilde{\sigma}^j \hat{g}_{\text{two}}^{W\dagger}. \tag{B5}
 \end{aligned}$$

Set

$$\begin{aligned}
 \rho & = \sum_{b,B,b',B'} |\psi_0^W(b,B)\rangle \rho_{b,B;b',B'} \langle \psi_0^W(b',B')| \\
 & = \hat{g}_{\text{two}}^W \tilde{\rho} \hat{g}_{\text{two}}^{W\dagger} \tag{B6}
 \end{aligned}$$

where $\tilde{\rho} = \sum_{b,B,b',B'} |b_0\rangle \rho_{b,B;b',B'} \langle b'_0| \langle B'_0|$. Define

$$\begin{aligned}
 e^{-1/\xi_{\text{two}}(\theta)} & = \frac{\text{Tr} \rho \left[\sum_{i,j=1}^3 \zeta^{ij} \tau^{ij} \right]}{9} \\
 & = \frac{\text{Tr} \left[\sum_{i,j=1}^3 \mathcal{W} \tilde{\sigma}^i \otimes \tilde{\sigma}^j \mathcal{W}^\dagger \hat{g}_{\text{two}}^W (\tilde{\sigma}^i \otimes \tilde{\sigma}^j \tilde{\rho}) \right]}{9} \\
 & = 1 - p_{\text{two}}(\theta) \tag{B7}
 \end{aligned}$$

using (A2).

APPENDIX C: GAPPED TO GAPLESS PHASE TRANSITION

In the main text, the gapped to gapless phase transition is discussed in the context of a specific family of circuits. This specific family is chosen for simplicity: all it does is form a Bell pair. However, the gapped to gapless phase transition occurs for any family of circuits with increasingly long-range entanglement in the output. We formalize this statement in this section, relying on the discussion in [16]. Then, we observe that the phase transition can actually occur more generically.

To begin, we need a definition of distance to capture the notion of long-range entanglement. Suppose we are given a circuit \mathbf{C} . Choose two of its qubits x and y . Define the distance between x and y as the minimum number of gates one must traverse to form a continuous line connecting the output of x and the output of y in the circuit diagram of \mathbf{C} . For example, in the family of Bell pair circuits discussed in the main text (see Fig. 5), x could refer to the first qubit and y to the second qubit. To connect the output of x and the output of y , we must traverse backward through G identity gates from the output of

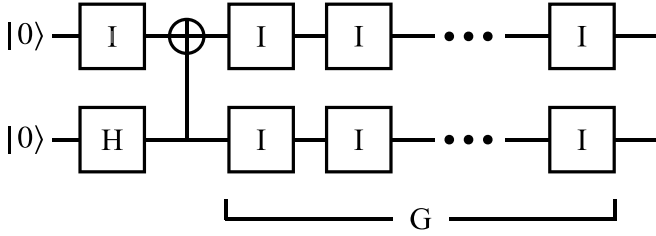


FIG. 5. Circuit that generates a Bell pair and then applies G identity gates to each member of the pair.

x to get to a CNOT gate, traverse the CNOT gate over to qubit y , and then traverse forward G identity gates to get to the output of y . Thus, the distance between x and y is $2G + 1$. If X and Y denote sets of qubits, define the distance between them as the minimum distance between any qubit x in X and any qubit y in Y .

Now, consider measuring a Hermitian operator $A_{X^C}^C$ on the output state of the circuit C . The subscript of $A_{X^C}^C$ indicates that it is supported on the set X^C of qubits of the circuit C . Similarly, consider measuring a Hermitian operator $B_{Y^C}^C$ that is supported on a set Y^C of qubits among the output of the circuit C . We can compute the distance between the sets X^C and Y^C in the manner described in the previous paragraph. We can also look for entanglement by computing the correlation $\langle A_{X^C}^C B_{Y^C}^C \rangle - \langle A_{X^C}^C \rangle \langle B_{Y^C}^C \rangle$ in the output state. For example, consider the fault-tolerant version of the Bell pair circuit of Fig. 5, in which each horizontal line is associated with a logical qubit and each gate with a logical gate. Choose X^C to be the set of physical qubits comprising the first logical qubit. Choose Y^C to be the set of physical qubits comprising the second logical qubit. Set $A_{X^C}^C$ to be the logical Z operator of the first logical qubit, appropriately dressed to handle physical bit-flip errors in the logical qubit [33]. Set $B_{Y^C}^C$ to be the dressed logical Z operator of the second logical qubit. Then, $\langle A_{X^C}^C B_{Y^C}^C \rangle - \langle A_{X^C}^C \rangle \langle B_{Y^C}^C \rangle$ is ≈ 1 independent of the value of G .

With this framework, we can consider the gapped to gapless phase transition. Suppose that we are given a linearly ordered set of circuits F . Suppose that we can identify an $A_{X^C}^C$ and $B_{Y^C}^C$ for each $C \in F$ such that the distance between X^C and Y^C grows as we proceed through F but the correlation always satisfies $\langle A_{X^C}^C B_{Y^C}^C \rangle - \langle A_{X^C}^C \rangle \langle B_{Y^C}^C \rangle \geq k$ for some constant k . For each circuit C , construct a Hamiltonian $H(\theta)$ and ground state $|\Psi(\theta)\rangle$ according to the mapping detailed in the main text. The condition $\langle A_{X^C}^C B_{Y^C}^C \rangle - \langle A_{X^C}^C \rangle \langle B_{Y^C}^C \rangle \geq k$ implies a corresponding correlation in $|\Psi(\theta)\rangle$, provided θ is sufficiently close to $\pi/2$. Given this correlation in the ground state, we can apply theorem 2.8 of [16]. This theorem indicates that, as we proceed through the set of circuits F , the gap of the Hamiltonians must shrink down to zero. Since it is easily seen by inspection that $H(\theta)$ is gapped near $\theta = 0$, there must be a gapped to gapless phase transition for F .

We have now demonstrated that a gapped to gapless phase transition occurs for any family of circuits with increasingly long-range entanglement among the output logical qubits. One wonders whether the long-range entanglement is essential: does a phase transition occur even in its absence? (For instance, perhaps the phase transition occurs simply as a result

of entanglement of the physical qubits within each individual logical qubit rather than entanglement between logical qubits.) To consider this, note that the gap of the Hermitian operator $H(\theta)$ is unaffected by the application of a unitary transformation. Thus, the phase transition would still occur if we were to start with a linearly ordered set of circuits F exhibiting long-range entanglement and then eliminate the long-range entanglement via unitary transformations on the Hamiltonians.

For an illustration of this idea, consider the fault-tolerant version of Fig. 5. We have established that the phase transformation occurs in this case. But, suppose that the logical CNOT gate were replaced with a two-qubit logical identity gate. Even though the circuit would no longer produce a Bell pair, there would still be a phase transition. To see this, note that the logical CNOT gate is simply a collection of transverse CNOT gates in the fault-tolerant construction of [5] on which we have relied. When we map the circuit to a Hamiltonian $H(\theta)$, each CNOT in this collection of transverse CNOT gates appears in $H(\theta)$ in the manner described in Fig. 2(d) and Eq. (A3). But it is possible to perform a unitary operation on $H(\theta)$ that transforms $W = \text{CNOT}$ in Eq. (A3) into a two-qubit identity gate. This unitary operation does not affect the gap of $H(\theta)$, so the gapped to gapless phase transition must still occur.

APPENDIX D: PEPS FORM OF THE GROUND STATE

Here, we show how the ground state $|\Psi(\theta)\rangle$ can be written as a projected entangled pair state. Rather than a formal proof, which would require the introduction of cumbersome notation, we consider the examples shown in Fig. 2. The general pattern will become clear from these examples.

In the case of Fig. 2(a), the ground state is a trivial projected entangled pair state: $|\Psi(\theta)\rangle = |0_0\rangle$. For Fig. 2(b), define the map

$$\begin{aligned} \hat{A} = & \cos \theta (|0_0\rangle\langle 0_0| + |1_0\rangle\langle 1_0|) \otimes (|0_1\rangle\langle 0_1| + |1_1\rangle\langle 1_1|) \\ & + \frac{1}{\sqrt{2}} \sin \theta (|\text{IDLE}\rangle\langle 0_0| \otimes |\text{IDLE}\rangle\langle 0_1| \\ & + |\text{IDLE}\rangle\langle 1_0| \otimes |\text{IDLE}\rangle\langle 1_1|). \end{aligned} \quad (\text{D1})$$

Then, the ground state $|\Psi(\theta)\rangle$ has the PEPS form

$$(I^{(2)} \otimes \hat{A})[(|0_0\rangle|0_0\rangle + |1_0\rangle|1_0\rangle) \otimes (\mathcal{U}|0_1\rangle + |0_0\rangle)] \quad (\text{D2})$$

up to normalization. In Fig. 2(c), $|\Psi(\theta)\rangle$ has the PEPS form

$$\begin{aligned} (I^{(2)} \otimes \hat{A} \otimes \hat{A})\{ & (|0_0\rangle|0_0\rangle + |1_0\rangle|1_0\rangle) \\ & \otimes [(\mathcal{V}|0_1\rangle + |0_0\rangle)|0_0\rangle + (\mathcal{V}|1_1\rangle + |1_0\rangle)|1_0\rangle] \\ & \otimes (\mathcal{U}|0_1\rangle + |0_0\rangle)\} \end{aligned} \quad (\text{D3})$$

up to normalization. Here, we have defined $\mathcal{V} = \sum_{b,\beta,s=0,1} |b_s\rangle\langle b|V|\beta\rangle\langle\beta_s|$ that applies V while keeping the stage fixed. If a circuit were to include more one-qubit gates, for each gate we would include another factor similar to the form $[(\mathcal{V}|0_1\rangle + |0_0\rangle)|0_0\rangle + (\mathcal{V}|1_1\rangle + |1_0\rangle)|1_0\rangle]$ and perform an additional projection using \hat{A} .

The final example, shown in Fig. 2(d), has a ground state of the form

$$(I^{(2)} \otimes \hat{A} \otimes I^{(2)} \otimes \hat{A}) \left[(|0_0\rangle|0_0\rangle + |1_0\rangle|1_0\rangle) \otimes |0_0\rangle \otimes (|0_0\rangle|0_0\rangle + |1_0\rangle|1_0\rangle) \otimes |0_0\rangle + \sum_{b', B'} \langle b' | \langle B' | W | 0 \rangle | 0 \rangle (|0_0\rangle|0_0\rangle + |1_0\rangle|1_0\rangle) \otimes |b'_1\rangle \otimes (|0_0\rangle|0_0\rangle + |1_0\rangle|1_0\rangle) \otimes |B'_1\rangle \right]. \quad (\text{D4})$$

The first term in brackets has both qubits in their initialized states $|0_0\rangle$ and $|0_0\rangle$. The second term in brackets has both qubits emerging from W in the states $|b'_1\rangle$ and $|B'_1\rangle$, with the transition matrix elements given by $\langle b' | \langle B' | W | 0 \rangle | 0 \rangle$. The projection operators \hat{A} take care of the teleportation circuits that act after W .

In these examples, we see the structure that characterizes $|\Psi(\theta)\rangle$ for any circuit. The unitary gates are included in the entangled pairs, and the projections are performed using \hat{A} .

-
- [1] P. W. Shor, Scheme for reducing decoherence in quantum computer memory, *Phys. Rev. A* **52**, R2493(R) (1995).
- [2] F. Gaitan, *Quantum Error Correction and Fault Tolerant Quantum Computing* (CRC Press, Boca Raton, FL, 2008).
- [3] *Quantum Error Correction*, edited by D. A. Lidar and T. A. Brun (Cambridge University Press, Cambridge, England, 2013).
- [4] J. Roffe, Quantum error correction: An introductory guide, *Contemp. Phys.* **60**, 226 (2019).
- [5] D. Aharonov and M. Ben-Or, Fault-tolerant quantum computation with constant error rate, *SIAM J. Comput.* **38**, 1207 (2008).
- [6] E. Knill, R. Laflamme, and W. Zurek, Resilient quantum computation, *Science* **279**, 342 (1998).
- [7] A. Y. Kitaev, Quantum computations: Algorithms and error correction, *Russ. Math. Surv.* **52**, 1191 (1997).
- [8] E. Dennis, A. Kitaev, A. Landahl, and J. Preskill, Topological quantum memory, *J. Math. Phys.* **43**, 4452 (2002).
- [9] A. Y. Kitaev, A. H. Shen, and M. N. Vyalyi, *Classical and Quantum Computation* (American Mathematical Society, Providence, 2000).
- [10] A. Mizel, M. W. Mitchell, and M. L. Cohen, Energy barrier to decoherence, *Phys. Rev. A* **63**, 040302(R) (2001).
- [11] A. Mizel, M. W. Mitchell, and M. L. Cohen, Scaling considerations in ground state quantum computation, *Phys. Rev. A* **65**, 022315 (2002).
- [12] A. Mizel, Mimicking time evolution within a quantum ground state: ground-state quantum computation, cloning, and teleportation, *Phys. Rev. A* **70**, 012304 (2004).
- [13] A. Mizel, Entanglement versus gap, quantum teleportation, and the AKLT model, *J. Phys.: Condens. Matter* **33**, 315801 (2021).
- [14] C. H. Bennett, G. Brassard, C. Crépeau, R. Jozsa, A. Peres, and W. K. Wootters, Teleporting an unknown quantum state via dual classical and Einstein-Podolsky-Rosen channels, *Phys. Rev. Lett.* **70**, 1895 (1993).
- [15] This example was pointed out to me by M. B. Hastings.
- [16] M. Hastings and T. Koma, Spectral gap and exponential decay of correlations, *Commun. Math. Phys.* **265**, 781 (2006).
- [17] B. Nachtergaele and R. Sims, Lieb-Robinson bounds and the exponential clustering theorem, *Commun. Math. Phys.* **265**, 119 (2006).
- [18] S. Hernandez-Santana, C. Gogolin, J. I. Cirac, and A. Acín, Correlation decay in fermionic lattice systems with power-law interactions at nonzero temperature, *Phys. Rev. Lett.* **119**, 110601 (2017).
- [19] Z.-X. Gong, M. Foss-Feig, F. G. S. L. Brandão, and A. V. Gorshkov, Entanglement area laws for long-range interacting systems, *Phys. Rev. Lett.* **119**, 050501 (2017).
- [20] D. Gosset and Y. Huang, Correlation length versus gap in frustration-free systems, *Phys. Rev. Lett.* **116**, 097202 (2016).
- [21] R. Cleve, D. Gottesman, and H.-K. Lo, How to share a quantum secret, *Phys. Rev. Lett.* **83**, 648 (1999).
- [22] E. M. Kessler, I. Lovchinsky, A. O. Sushkov, and M. D. Lukin, Quantum error correction for metrology, *Phys. Rev. Lett.* **112**, 150802 (2014).
- [23] I. Rojko, D. Layden, P. Cappellaro, J. Home, and F. Reiter, Bias in error-corrected quantum sensing, *Phys. Rev. Lett.* **128**, 140503 (2022).
- [24] Z. Huang, G. K. Brennen, and Y. Ouyang, Imaging stars with quantum error correction, *Phys. Rev. Lett.* **129**, 210502 (2022).
- [25] T. Yamakawa and M. Zhandry, Verifiable quantum advantage without structure, in *Proceedings of the 2022 IEEE 63rd Annual Symposium on Foundations of Computer Science (FOCS)* (IEEE, Piscataway, NJ, 2022), pp. 69–74.
- [26] J. I. Cirac, D. Perez-García, N. Schuch, and F. Verstraete, Matrix product states and projected entangled pair states: Concepts, symmetries, theorems, *Rev. Mod. Phys.* **93**, 045003 (2021).
- [27] N. Schuch, M. M. Wolf, F. Verstraete, and J. I. Cirac, Computational complexity of projected entangled pair states, *Phys. Rev. Lett.* **98**, 140506 (2007).
- [28] G. Scarpa, A. Molnar, Y. Ge, J. J. Garcia-Ripoll, N. Schuch, D. Perez-García, and S. Iblisdir, Projected entangled pair states: Fundamental analytical and numerical limitations, *Phys. Rev. Lett.* **125**, 210504 (2020).
- [29] Z.-Y. Wei, D. Malz, and J. I. Cirac, Sequential generation of projected entangled-pair states, *Phys. Rev. Lett.* **128**, 010607 (2022).
- [30] M. Fannes, B. Nachtergaele, and R. F. Werner, Finitely correlated states on quantum spin chains, *Commun. Math. Phys.* **144**, 443 (1992).
- [31] M. J. Kastoryano, A. Lucia, and D. Perez-García, Locality at the boundary implies gap in the bulk for 2D peps, *Commun. Math. Phys.* **366**, 895 (2019).
- [32] T. Albash and D. A. Lidar, Adiabatic quantum computation, *Rev. Mod. Phys.* **90**, 015002 (2018).
- [33] H. Bombin, R. W. Chhajlany, M. Horodecki, and M. A. Martin-Delgado, Self-correcting quantum computers, *New J. Phys.* **15**, 055023 (2013).